Available online at www.sciencedirect.com
ScienceDirect
Solid State Sciences 8 (2006) 1138–1143
Solid State Sciences
www.elsevier.com/locate/ssscie

The role of covalency in the orbital-order of $3d^1$ perovskites

S. Leoni [a,*], L. Craco [b], A. Ormeci [a], H. Rosner [a]

[a] *Max-Planck-Institut für Chemische Physik fester Stoffe, Nöthnitzer Str. 40, 01187 Dresden, Germany*
[b] *Institut für Theoretische Physik, Universität zu Köln, 50937 Köln, Germany*

Received 21 February 2006; received in revised form 4 April 2006; accepted 7 May 2006

Available online 9 August 2006

Abstract

We investigate the interplay between lattice distortion, bond formation and orbital ordering in $ATiO_3$ (A = La, Y) perovskites using full-potential density-functional calculations and ELF analysis. It is shown that the lattice distortion implies a dramatic reorganization of the bonds between A cations and oxygen on the one hand, and titanium and oxygen on the other hand. Along the series cubic $LaTiO_3$, orthorhombic $LaTiO_3$, orthorhombic $YTiO_3$ an increasing asymmetrization of the environment of Ti is taking place.

We show that changes in chemical bonding are relevant for lifting the degeneracy of Ti 3d orbitals across the metal–insulator transition and we sketch the use of the ELF to visualize orbital ordering.

1. Introduction

Perovskite titanates $ATiO_3$ with A-dependent lattice distortion (A = La, Pr, Nd, Sm, Y, ...) [1,2] are classic examples of a system exhibiting Mott–Hubbard insulator–metal transition [3,4] that is driven by doping. The insulating ground state in these fascinating systems can vary from ferromagnetic [4] to G-type antiferromagnetic insulators [2] with ferro-orbital order. Here, orbital degrees of freedom play an important role, strongly determining the magnetic properties of the system. The underlying microscopic mechanism, leading to different magnetic responses in these compounds, is still an open problem, despite of many recent efforts [2,5,6].

The deviation of the crystal structure of $ATiO_3$ compounds from the cubic symmetry is caused by a $GdFeO_3$-type distortion. The magnitude of this distortion correlates with the ionic radius, r, of the interstitial A ion. With a small r the lattice is more distorted and the Ti–O–Ti bond angle deviates from 180°. Classical examples, considered in this work, are $LaTiO_3$ ($r_{La} = 1.17$ Å) and $YTiO_3$ ($r_Y = 1.04$ Å). In $LaTiO_3$ the bond angle is 157° in the ab plane (*Pbnm* setting) and 156° along the c axis. In $YTiO_3$ the angles are 144° (ab plane) and 140° (c axis). With increasing $GdFeO_3$-type distortion, the Néel temperature decreases and ferromagnetic order sets in [2].

The Jahn–Teller (JT) distortion is also present in perovskite lattices. There exist two different types of JT distortions depending on the stacking of the elongated octahedra along the c axis [5]. Type a distortion is characterized by alternatingly elongated octahedra, type d by octahedra elongated in the same way along the c axis. In the early transition-metal oxides the JT distortion is small, the related crystal field splitting has almost cubic symmetry.

Clearly, if the crystal field has cubic symmetry then the degeneracy of the t_{2g} orbitals is not lifted. Recent crystallographic measurements by Cwik et al. [7] have refined the earlier data, concluding that orbital degeneracy is lifted in the ground state of the JT distorted $LaTiO_3$. According to the interpretation of Ref. [6], the JT effect in $LaTiO_3$ is caused by differences between the O–O bond lengths rather than by Ti–O ones. Furthermore, neutron diffraction by Akimitsu et al. [8] shows that orbital order (i.e., the alternation of occupied orbitals at different atomic sites) in the ferromagnetic insulating state of $YTiO_3$ is compatible with d-type JT distortion ($TiO_{6/2}$ octahedra elongation along the c axis).

Several first-principles methods have been used to investigate orbital and spin orientations in $3d^1$ perovskite titanates [9–11]. LDA and GGA failed to reproduce both the G-type antiferromagnetic structure of $LaTiO_3$ as well as its insu-

* Corresponding author. Tel.: +49 351 46462270; fax: +49 351 46463002.
E-mail address: leoni@cpfs.mpg.de (S. Leoni).

1293-2558/$ – see front matter
doi:10.1016/j.solidstatesciences.2006.05.016

lating ground state. This is related to the fact that strong electron–electron interactions, which determine the low energy physics of this system [12], are not accounted for sufficiently in standard approximation schemes to the density-functional theory (LDA, GGA). The G-type antiferromagnetic structure of $LaTiO_3$ is also not correctly obtained within LDA + U calculations [13], indicating the dynamical nature of electron–electron interactions. In spite of that, first-principles methods are powerful tools in providing the general trend of spatial electron distribution on different atoms [10,11].

To account for the orbital ordering patterns seen in polarized neutron diffraction experiments [8], the resulting charge density is usually shown in three-dimensional drawings. As expected for $LaTiO_3$ and $YTiO_3$, near the Fermi level the charge density has predominantly t_{2g} character. According to GGA and GGA + U calculations [11], these titanates show different types of orbital ordering. Results from [11] seem to indicate that the ground state orbital (GSO) in the La-based compound does not point towards the O-atoms. Given the fact that the JT distortion is small in $LaTiO_3$, orbital order is therefore driven predominantly by rotations and tiltings of the $TiO_{6/2}$ basic structure.

On the other hand, the elongation of the GSO towards oxygen atoms is seen in $YTiO_3$, which may induce distortions on the $TiO_{6/2}$ octahedra as well.

In the following we shall investigate the effect of the $GeFeO_3$ type distortion on the bonding, elucidating the interplay between structural distortion inducing orbital order and bond formation [14]. We will show that in a situation where orbital fluctuations are suppressed by a local distortion, the orbital orientation at each site strictly follows the symmetry imposed by the local crystal field.

2. Method

The electron localization function (ELF) is a widely used tool to study chemical bonding in molecules and solids [15]. The ELF monitors the correlation of the movement of parallel spin electrons in real space [16]. In this study the ELF calculations were performed by using the ELF module as implemented [17] in the all-electron, full-potential local orbital (FPLO) minimal basis method [18]. In FPLO each atomic orbital nl with principal quantum number n and angular momentum l is represented by one basis function only. The basis functions are obtained by solving an effective Schrödinger equation which contains the spherically averaged crystal potential and an artificial confining potential [19]. The confining potential makes the basis functions more strongly localized than the atomic orbitals. The FPLO method does not have any atomic (or muffin–tin) spheres so that the whole space is treated in a uniform manner.

In the scalar relativistic calculations within the LDA scheme (Perdew and Wang [20]) La(4s, 4p, 4d, 5s, 5p, 6s, 6p, 5d), Y(3d, 4s, 4p, 5s, 5p, 4d), Ti(3s, 3p, 4s, 4p, 3d) and O(2s, 2p, 3d) represented the basis sets. Lower-lying states were treated as core states. 3d, 4s, 4p (Y), 4s, 4p, 4d (La), 3s, 3p (Ti) states were included in the basis sets to avoid occurrence of core-core overlaps. A k mesh of 84 (cubic structures) and 512 (orthorhombic structures) irreducible points in the Brillouin zone ensured convergence with respect to the number of k-points. The spatial extension of the orbitals forming the basis was optimized to minimize the total energy. For the ELF calculation meshes of 77 652 (cubic) and 812 437 (orthorhombic) irreducible points were used. The orthorhombic structural parameters were chosen in the *Pnma* setting.

3. Results

In the LDA DOS of the real ($GdFeO_3$-type distorted) structures of $LaTiO_3$ and $YTiO_3$ (Fig. 1) the Ti 3d states are found around the Fermi level (Figs. 2(a), (b), upper part), 5d La (4d Y) and Ti 3d states hybridize with O 2p states. With respect to the DOS of the idealized cubic structures (Figs. 2(a), (b), lower part), the distortion has widened the splitting between t_{2g} and e_g states. Furthermore, the La (Y) states have been shifted in energy, and the La (Y) and Ti band widths have become narrower, hinting at changes in the bonding situation of the structures.

3.1. Cubic $LaTiO_3$

To better follow the changes in the bonding caused by the distortion, we have calculated the ELF for $LaTiO_3$ and $YTiO_3$ in the idealized cubic structure (Fig. 3(a)). At ELF value $\eta = 0.83$ the Ti outer-core shell shows a pronounced structuring. Interestingly, the isosurface is not spherical anymore (like it would be for an isolated atom) [21], hinting at an interaction with oxygen atoms. The shell is punctured at six places instead, along the shortest Ti–O contacts inside the Ti-centered oxygen octahedron. On increasing $\eta(0.84)$, the structured shell separates into eight localization domains, pointing towards the faces of the octahedron (Fig. 3(a), white isosurface). The valence shell of oxygen separates into two localization domains ($\eta = 0.85$), placed along Ti–O contacts, on the edges of the cubic unit cell and within the octahedra (Fig. 3(a), white isosurface). The outer-core shell of La shows punctures along the shortest 12 La–O contacts (Fig. 3(a), orange isosurface), at $\eta = 0.75$. Integration of the electronic density in the ELF basins [22] yields charges of 2.5+ for Ti, 2.3+ for La and 1.6− for O. These values deviate significantly from the integer count expected for ionic compounds. Together with the structuring of the La and Ti outer-core shells, and of the valence shell of oxygen, this is a signature of La–O and Ti–O covalent bonds.

3.2. Orthorhombic $LaTiO_3$

In orthorhombic $LaTiO_3$ the octahedra are rotated around the (former cubic) O1–Ti–O1 axis and tilted away from the b axis (*Pnma* setting, c axis in *Pbnm*). This causes the formation of shorter La–O contacts. The structuring of the outer-core shell of La in the ELF is correspondingly pronounced. The deviation from spherical shells results in a structuring that hints at oriented La–O bonds. The number of punctures is 4 now ($\eta = 0.71$), along shortest La–O contacts. Each O1 oxygen (light blue in Fig. 3(b)) has two different bonds to two La atoms (2.423 and 2.536 Å), O2 atoms (dark blue, Fig. 3(b)) are bound

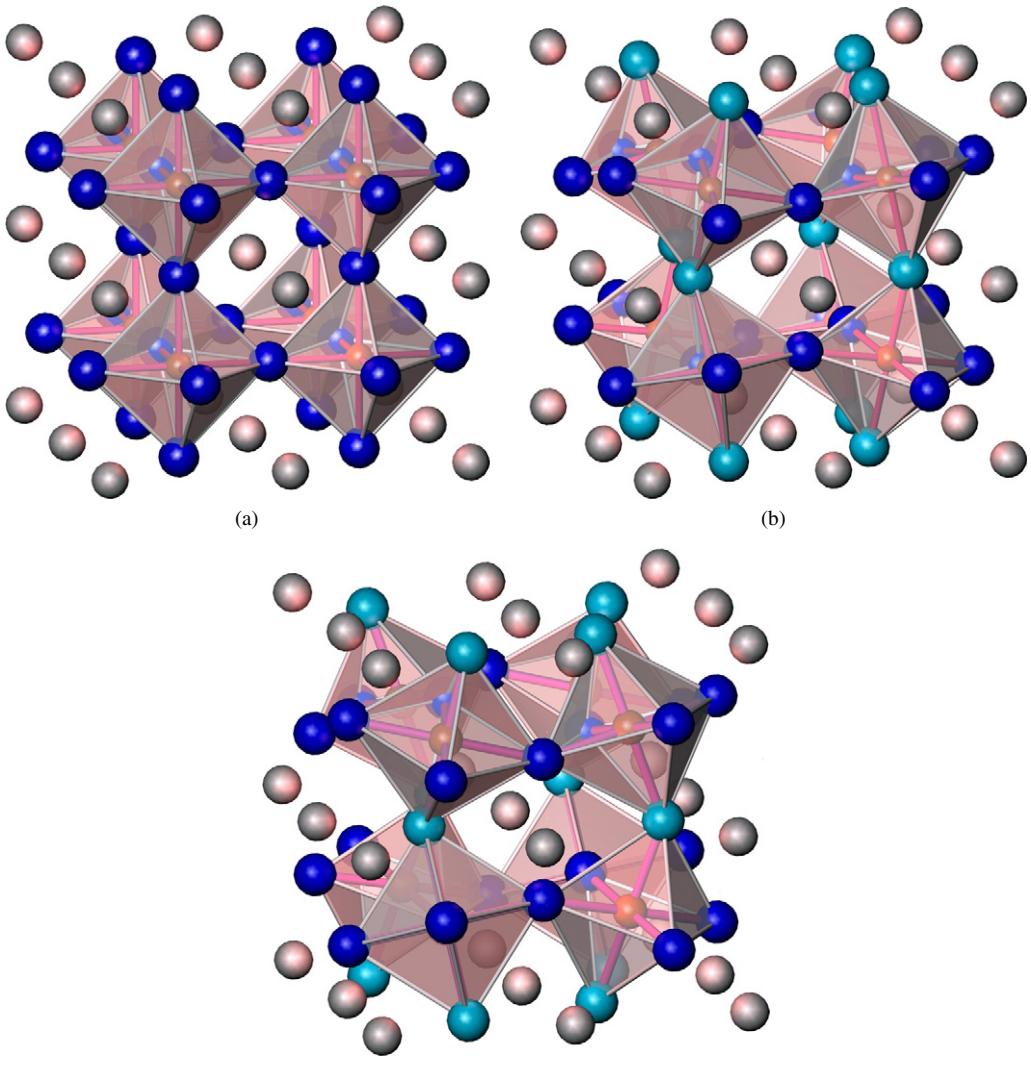

Fig. 1. (a) Idealized cubic structure of $LaTiO_3$ ($YTiO_3$). (b) Real structure of $LaTiO_3$, orthorhombic Pnma. (c) Real structure of $YTiO_3$, orthorhombic, Pnma. La and Y are grey, Ti is orange, O is blue (cubic structures), O1 is light blue and O2 is blue (orthorhombic structures).

to only one La atom each (2.451 Å, next La at 2.669 Å). The valence shell of O1 ($\eta = 0.84$) is also punctured, such that it appears as a torus-like double shell around O1 (Fig. 4(a)). At $\eta = 0.845$ localization domains are found on the external Ti–O1–Ti angle, outside of the $TiO_{6/2}$ octahedra. A torus-like double shell is also found around O2 atoms ($\eta = 0.84$). At higher η, localization domains appear on the external Ti–O2–Ti angle, as well as along Ti′–O2–Ti connections. The decomposition of the double shell is not symmetric along Ti′–O2–Ti connections (Ti′ and Ti are the centers of corner-connected octahedra), hinting at different Ti′–O2 and Ti–O2 bonds.

The stronger interaction with La, visible in the formation of fewer oriented covalent bonds, has thus made the oxygen atoms different. This correlates with the Ti–O bonds elongation in the order Ti–O1 ≈ Ti′–O2 < Ti–O2.

The changes of the Ti–O bonds appear clearly in the ELF. At $\eta = 0.84$ the outer-core shell of Ti consists of two localization domains along [110], and a torus aligned with it (Fig. 4(a), frontal octahedron, white isosurface). The shell of Ti shows two different, alternating orientations along the *b* axis (*Pnma* setting), [110] and [−110] (Fig. 4(a), within the octahedra). The structuring of the Ti shells reflects thus the local changes of the crystal field and of the bonding situation.

3.3. Orthorhombic $YTiO_3$

In $YTiO_3$ the rotation and tilting of the octahedra have further increased. The formation of oriented Y–O bonds is again clearly identified in the ELF. At $\eta = 0.79$ the outer-core shell of Y is strongly structured, and punctures are present in the direction of oxygen atoms (Fig. 3(c)). Each O1 atom is in closer contact to one plus one Y atoms (2.222 Å + 2.313 Å), O2 are bound to one Y atom (2.280 Å, next Y at 2.508 Å).

The localization domains of the O1 valence shell ($\eta = 0.84$) are found outside of the $TiO_{6/2}$ octahedron, on the external Ti–O1–Ti angle. The difference in the position of the localization domains of the valence shell of O2 ($\eta = 0.84$) along Ti′–O2–Ti connections is even more pronounced with respect to $LaTiO_3$. One of the two pairs of equivalent bonds is longer, and the

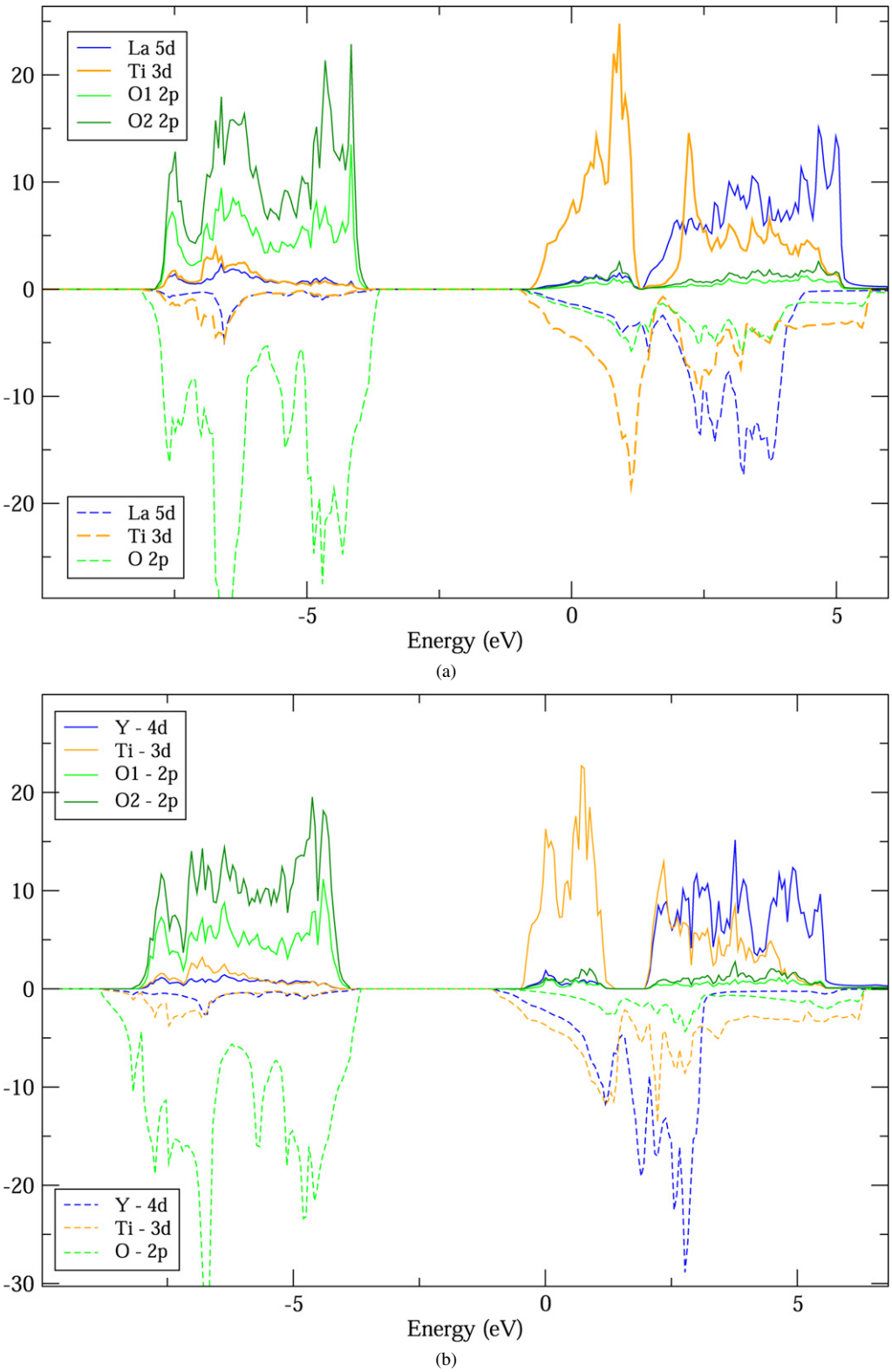

Fig. 2. (a) LDA DOS of $LaTiO_3$. Upper part, real structure. Lower part, idealized cubic structure. (b) LDA DOS of $YTiO_3$. Upper part, real structure. Lower part, idealized cubic structure.

bond lengths increase in the order Ti′–O2 ≈ Ti–O1 < Ti–O2. The oxygen environment of Ti has thus become even more asymmetric with respect to the ideal cubic structures, as a consequence of Y–O oriented bonds and changes in the Ti–O bonds. The ELF around Ti ($\eta = 0.84$) shows six localization domains (Fig. 4(b)). Similar to the case in $LaTiO_3$ two domains are aligned close to the [110] direction, again alternating with [−110] along the *b* axis (*Pnma* setting), the other four are arranged in a ring (Fig. 4(b), corresponds to the torus-like shape in $LaTiO_3$). In the *ac* plane, two orientations are possible, that

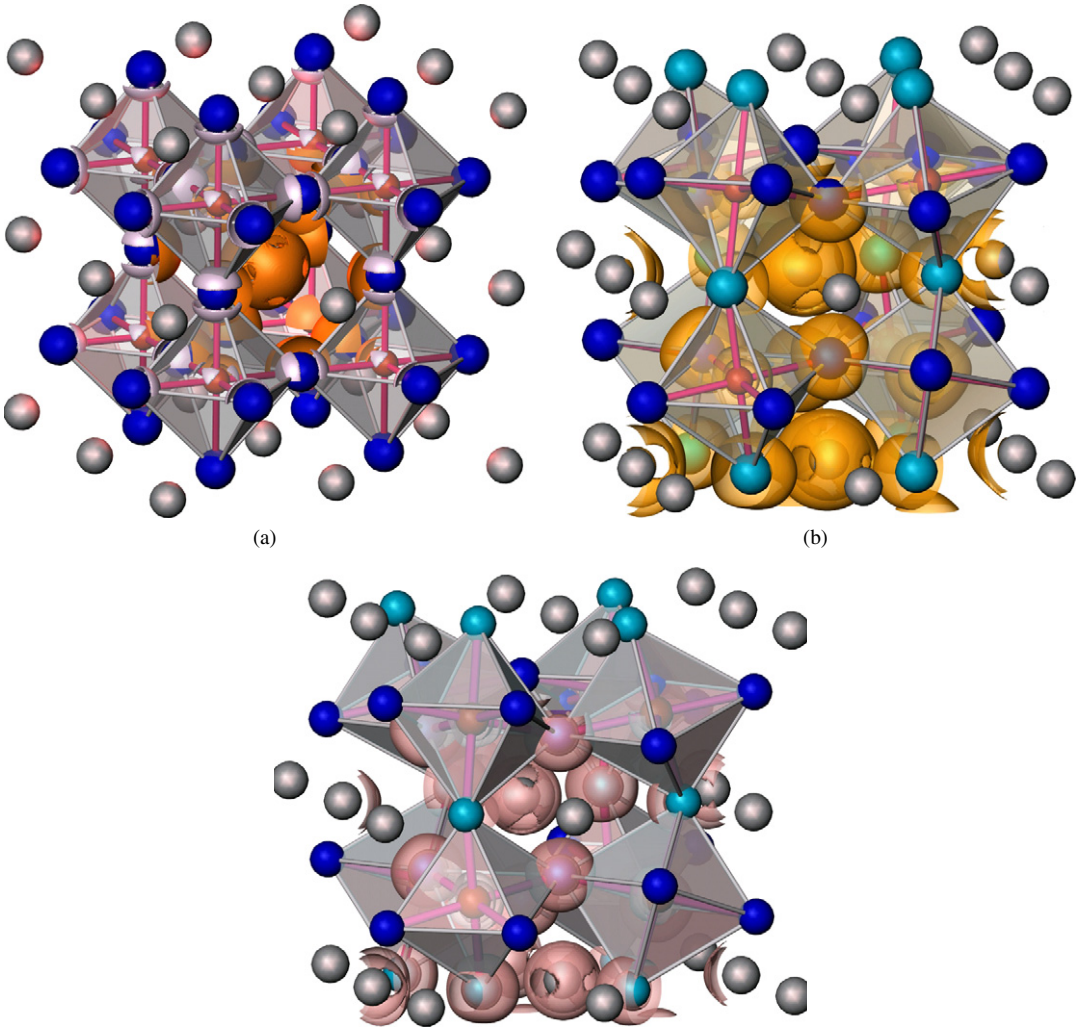

(a) (b)

(c)

Fig. 3. (a) ELF of $LaTiO_3$ in the idealized cubic structure. Orange isosurface for $\eta = 0.74$, white isosurface for $\eta = 0.84$. (b) ELF for $LaTiO_3$ in the orthorhombic structure, Pnma. Isosurface for $\eta = 0.71$. (c) ELF for $YTiO_3$ in the orthorhombic structure. Isosurface for $\eta = 0.79$.

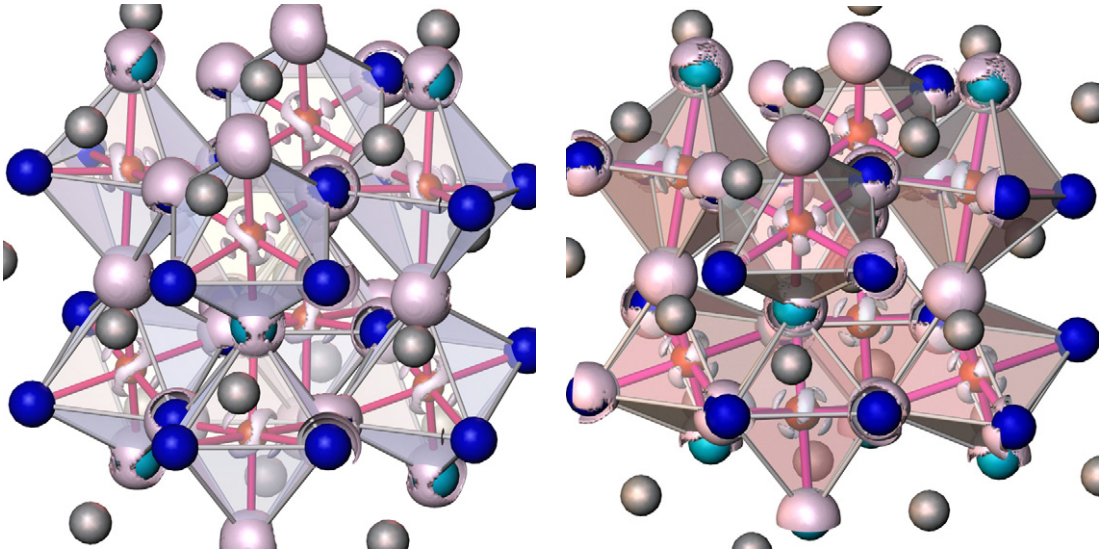

(a) (b)

Fig. 4. (a) ELF for orthorhombic $LaTiO_3$. Isosurface for $\eta = 0.84$. The alternating orientation of the structured Ti shell along the *b* axis are displayed (*Pnma* setting, *b* axis vertical). (b) ELF for orthorhombic $YTiO_3$. Isosurface for $\eta = 0.84$. The different orientation of the structured Ti shell in the plane and along the *b* axis (vertical) are displayed.

alternate along Ti′–O2–Ti connections, and that imply a 90° rotation in the local frame (Fig. 4(b)). The changes in the local symmetry, crystal field and bonds are again reflected in the ELF.

4. Discussion

The formation of a set of La–O and Y–O oriented bonds accompanies the $GdFeO_3$ distortion of $LaTiO_3$ and $YTiO_3$ from the cubic symmetry. The involvement of oxygen in the bonds changes the Ti environment. The ELF shows a clear change in the structuring of both the valence shell of oxygen atoms, and the outer-core shell of Ti atoms. The geometric deviation of the octahedra from that in the regular cubic structure is rather small, which may be insufficient to fully lift the degeneracy of Ti 3d orbitals. An asymmetry is introduced around Ti on distorting the structure through the bonding. The onset of La–O (Y–O) bonds, and the changes of the Ti–O bonds within the octahedra are clearly traced by the ELF. Furthermore, the deformation of the Ti shell and its site-dependent orientation in the distorted structures follows in a strict way the local changes of the crystal field and of the bonds. This feature corresponds to what in the language of orbital is called orbital ordering and reflects the changes in the crystal field.

The ELF calculations within the LDA approximation underline a covalent framework that becomes gradually distorted along the series cubic $LaTiO_3$, $LaTiO_3$, $YTiO_3$ and that accompanies the gap widening in the 3d manifold. Recent works [12,23,24] treat the electronic correlation within a LDA + DMFT scheme. Therein the paramagnetic Mott–Hubbard insulating state is correctly accounted for, while features already present in the LDA calculations, like the coefficients of the expansion of the ground state wave function in the local t_{2g} orbitals are only slightly corrected. This supports the robustness of the covalent framework as emerging at the LDA level and its role in the overall distortion.

5. Conclusions

In this work we have performed full-potential ELF calculations of $LaTiO_3$ and $YTiO_3$, in the idealized and real ($GdFeO_3$-type distorted) structures. The ELF results show that the distortion is associated with dramatic changes in the covalent La–O (Y–O) and Ti–O bonds. Such changes, more than the small geometric changes of the oxygen geometry around Ti, are responsible for the lifting of the degeneracy of Ti 3d orbitals. Furthermore, the oriented character of the Ti outer-core shell reflects the local changes of the crystal field. This is consistent with the picture of orbital ordering.

Acknowledgements

S.L. wishes to thank the Swiss National Foundation for financial support. The work of L.C. was carried out under the auspice of SFB 608 of the Deutsche Forschungsgemeinschaft. A.O. and H.R. acknowledge the Emmy-Noether-Programm of the Deutsche Forschungsgemeinschaft for funding. Fruitful discussions with Miroslav Kohout are gratefully acknowledged.

References

[1] G. Amow, J.-S. Zhou, J.B. Goodenough, J. Solid State Chem. 154 (2000) 619.
[2] M. Mochizuki, M. Imada, J. Phys. Soc. Japan 73 (2004) 1833.
[3] M. Imada, A. Fujimori, Y. Tokura, Rev. Mod. Phys. 70 (1998) 1039.
[4] K. Morikawa, T. Mizokawa, A. Fujimori, Y. Taguchi, Y. Tokura, Phys. Rev. B 54 (1996) 8446;
T. Katsufuji, Y. Taguchi, Y. Tokura, Phys. Rev. B 56 (1997) 10145.
[5] T. Mizokawa, A. Fujimori, Phys. Rev. B 54 (1996) 5368;
T. Mizokawa, D.I. Khomskii, G.A. Sawatzky, Phys. Rev. B 60 (1999) 7309;
I.V. Solovyev, Phys. Rev. B 69 (2004) 134403.
[6] R. Schmitz, O. Entin-Wohlman, A. Aharony, A.B. Harris, E. Müller-Hartmann, Phys. Rev. B 71 (2005) 144412, cond-mat/0506328.
[7] M. Cwik, et al., Phys. Rev. B 68 (2003) 060401.
[8] J. Akimitsu, et al., J. Phys. Soc. Japan 70 (2001) 3475.
[9] H. Fujitani, S. Asano, Phys. Rev. B 51 (1995) 2098;
M. Takahashi, J.-I. Igarashi, Phys. Rev. B 64 (2001) 075110;
S.V. Streltsov, et al., Phys. Rev. B 71 (2005) 245114.
[10] H. Sawada, K. Terakura, Phys. Rev. B 58 (1998) 6831.
[11] S. Okatov, A. Poteryaev, A. Lichtenstein, Europhys. Lett. 70 (2005) 499.
[12] L. Craco, M.S. Laad, S. Leoni, E. Müller-Hartmann, Phys. Rev. B 70 (2004) 195116.
[13] I. Solovyev, N. Hamada, K. Terakura, Phys. Rev. B 53 (1996) 7158.
[14] J.B. Goodenough, Magnetism and the Chemical Bond, Wiley, New York, 1963.
[15] A.D. Becke, K.E. Edgecombe, J. Chem. Phys. 92 (1990) 5397;
A. Savin, O. Jepsen, J. Flad, O.K. Andersen, H. Preuss, H.G. von Schnering, Angew. Chem. 104 (1992) 186;
A. Savin, O. Jepsen, J. Flad, O.K. Andersen, H. Preuss, H.G. von Schnering, Angew. Chem. Int. Ed. 31 (1992) 187.
[16] M. Kohout, Int. J. Quantum Chem. 97 (2004) 651.
[17] A. Ormeci, H. Rosner, F.R. Wagner, M. Kohout, Yu. Grin, J. Phys. Chem. A 110 (2006) 1100.
[18] K. Koepernik, E. Heschrig, Phys. Rev. B 59 (1999) 1743.
[19] H. Eschrig, Optimized LCAO Methods and the Electronic Structure of Extended Systems, Springer, Berlin, 1989.
[20] J.P. Perdew, Y. Wang, Phys. Rev. B 45 (2002) 13244.
[21] M. Kohout, F.R. Wagner, Yu. Grin, Theor. Chem. Acc. 108 (2002) 150.
[22] M. Kohout, Program basin, version 3.1, MPI für Chemische Physik fester Stoffe, Dresden, 2005.
[23] E. Pavarini, et al., Phys. Rev. Lett. 92 (2004) 176403.
[24] L. Craco, S. Leoni, E. Müller-Hartmann, in preparation.